Journal of Ceramic Processing Research. Vol. 18, No. 11, pp. 767~776 (2017)

J O U R N A L O F
Ceramic Processing Research

The friction and wear characteristics of SiC ceramics heat treated at high temperature

Seok-Hwan Ahn[a] and Ki-Woo Nam[b,*]

[a]*Department of Aero Mechanical Engineering, Jungwon University, Chungbuk, Korea*
[b]*Department of Materials Science and Engineering, Pukyong National University, Busan 48547, Korea*

Ceramics are used in a wide range of applications, both in lubricated and unlubricated contacts. Due to their hardness and high wear resistance to extensive usage, ceramics are used in many applications. In all cases, they must have excellent tribological characteristics. Silicon carbide composite ceramics were sintered, and friction and wear characteristics were evaluated at various specimen conditions. The SiC ceramics mainly had abrasive, adhesive and plowing wear during the dry sliding. All the specimens decreased concerning their friction coefficient and wear loss with increasing heat treatment temperature. The friction of heat treated as-received specimens at high temperature was more reduced than that of heat treated as-received specimens. The higher the heat treatment temperature and the longer the time, the thicker the SiO_2 oxide that was formed on the surface. In addition, the friction coefficient was smaller due to the lubrication action, but the wear loss was larger.

Key words: SiC ceramics, Friction coefficient, Wear loss, SiO_2 oxide, Debris.

Introduction

Ceramic has a variety of beneficial properties such as high hardness and strength, excellent thermal stability corrosion resistance, high thermal conductivity and low thermal expansion coefficient. It has been widely used for tribological applications like bearings, cylinder liners and mechanical seals. Friction arises as a resistance to motion when a solid surface moves over another surface. The surfaces of two bodies that slide against each other are subjected to high local stresses and pressures. This phenomenon results in local shear deformation and fracture of the surfaces, and locally high temperatures can also arise. There are studies in which the friction coefficient decreases when a locally high temperature occurs [1, 2]. Wear resistance greatly affects the driving and operating efficiency of a mechanical device. Indeed, about 30% of the energy is lost in the friction and wear process, which is closely related to productivity. Wear resistance studies are active because they are directly related to energy saving [3-6]. But the characteristics of wear resistance are not a unique characteristic of the material. Experimental results are influenced by the kind of counterpart materials and test conditions in place. In addition, it is difficult to obtain reproducible results because it is necessary to comprehensively be investigated not only the wear but also the lubrication and friction [7].

Ceramics are used in a wide range of applications, both in lubricated and unlubricated contacts [8, 9]. Due to their hardness and high wear resistance, ceramics are often used in applications such as metal cutting tool inserts, drawing dies, roller bearings, water pumps, and automotive engine parts, etc. In all these cases, excellent tribological characteristics are required. Alumina (Al_2O_3), zirconia (ZrO_2), silicon carbide (SiC) and silicon nitride (Si_3N_4) are the most common sintered ceramics used for engineering applications. However, alumina has low fracture toughness, which means that countless cracks may be initiated at random by heavy machining. Moreover, these cracks are too small to be detected by the latest non-destructive inspection techniques. Thus, there can be a considerable decrease in the mechanical properties, including the reliability of the ceramic component [10]. The most effective method to overcome these problems is to endow ceramics with a crack-healing ability. Crack-healing ability is a function by which the material detects surface cracks and heals them itself. This can be obtained by heat-treatment of SiC-containing ceramics. This is because the strength of the SiC-containing ceramic is increased by the heat treatment [11-21]. The heat treatment improves the strength, but the surface is oxidized [18]. There are no studies which investigate how this oxidation phenomenon affects friction and wear.

In this study, silicon carbide composite ceramics were sintered. The friction and wear characteristics were evaluated according to the heat treatment condition and the surface roughness. The specimens used are as follows. ① Heat treated specimens from

*Corresponding author:
Tel : +82-51-629-6358
Fax: +82-51-629-6353
E-mail: namkw@pknu.ac.kr

900 to 1200 °C to obtain optimum bending strength. ② After heat treatment for 1 hr at 1100 °C of optimum temperature, heat treated specimens for 10 minutes at each temperature from 900 to 1200 °C. ③ Heat treated surface roughness specimens for 1, 3 and 10 hrs at 1100 °C of optimum temperature.

Materials and Experimental Method

Commercially available SiC (Ultrafine grade, Ibiden Co., Japan), Al_2O_3 (AKP-700, Sumitomo Chemical Co. Ltd., Japan), Y_2O_3 (CI Chemical Co., Japan), and SiO_2 (CI Chemical Co., Japan and NGE Tech. Co., Korea) were used as the starting materials. The mean particle sizes of the SiC, Al_2O_3, Y_2O_3 and SiO_2 powders were 0.27 μm, 0.1 μm, 33 nm and 25 nm, respectively. The SiO_2 powder was added in order to evaluate the friction and wear characteristics according to the heat treatment. The powders were mixed in isopropanol for 24 hours using a SiC ball (φ5). The mixtures were subsequently hot-pressed in N_2 gas for one hour via hot-pressing conducted under 35 MPa at 1780 °C. The density of the specimens was obtained using the Archimedes principle.

Heat treated as-received specimens (SAY(AH), SAYS(AH)) in the air were one hour at various temperatures ranging from 900 to 1200 °C. The high temperature heat treated as-received specimens (SAY(HH), SAYS(HH)) were maintained for 1 hour at 1100 °C of an optimum temperature, and were maintained for 10 minutes at each temperature from 900 to 1200 °C. In order to compare the wear characteristics with the mirror polished specimen, the surface roughness specimens (SAY (R), SAYS (R)) were maintained for 1, 3 and 10 hours at 1100 °C of the optimum temperature of the heat treated as-received specimens. All cooling was spontaneous in the furnace. The compositions, sintering and heat treatment conditions of each specimen are shown in Table 1. Here, the average roughness of the mirror polished specimens is Ry = 0.04 μm, and the average roughness of the roughness specimen is Ry = 16.39 μm.

The type of wear machine was a “block on ring”. This equipment consists of a ring-shaped circular plate counterpart material which rotated during the test, and a rectangular-shaped specimen which was under a constant load in order to keep contact with the counterpart material. The counterpart material was SKD 11 with Φ35 and a thickness of 7 mm. The test conditions were as follows: (1) the rotation speed of the ring which has a dimension of 35 mm was 50 rpm; (2) the load was 9.8 N; (3) the total wear distance was 500 m; and (4) the tests were performed at room temperature in a dried condition.

To obtain a high reliability, 55,000 data which were obtained at 10 data per second were used. After the wear test, the worn surface, longitudinal section, wear debris of samples and worn surface of counter faces were characterized using a scanning electron microscope (SEM, VEGAII XMU, Tescan, Czech) coupled with an energy dispersive spectroscopy detector (EDX, INCA,).

Results and Discussion

Figs. 1-3 show the optical microscope images of the specimens after wear testing. Fig. 1 is SAY(AH) and SAY(HH), Fig. 2 is SAYS(AH) and SAYS(HH), Fig. 3 is SAY(R) and SAYS(R). The counterpart materials were difficult to find worn part. However, the specimens were able to clearly identify the wear areas as shown in the Figure. Based on the fact that scratches and small dent marks in one direction are observed on the worn part, the worn part shows abrasive wear behavior. The abrasive wear is the main mechanism, which is caused by micro-shear, which accounts for about 50% of the causes of wear loss.

Ten pieces of data, such as the wear coefficient, the wear loss, etc. was stored every second by a wear tester. Fig. 4 shows the representative data of the wear coefficient and wear loss from the wear tester. The X-axis is the wear distance, and the Y-axis is the wear coefficient and the wear loss, respectively. It can be seen that the coefficient of friction increases sharply at the beginning, and then the curve becomes flat. As this result demonstrates, the coefficient of friction is obtained by straightening a constant region that appears

Table 1. Batch composition and processing conditions.

Specimen	Batch composition (wt.%)	Processing conditions			Relative density (%)
		Hot-pressing (HP)	Crack-healing conditions		
			Polished specimen	Non-polished specimen	
SAY	90% SiC-6% Al_2O_3-4% Y_2O_3	35 MPa, 1780 °C, 1 hr, N_2	900 ~ 1300 °C, 1 hr, in air	1100 °C, 1 ~ 10 hr, in air	98.3
SAYS	85% SiC-7.2% Al_2O_3-4.8% Y_2O_3-3% SiO_2 powder				98.9

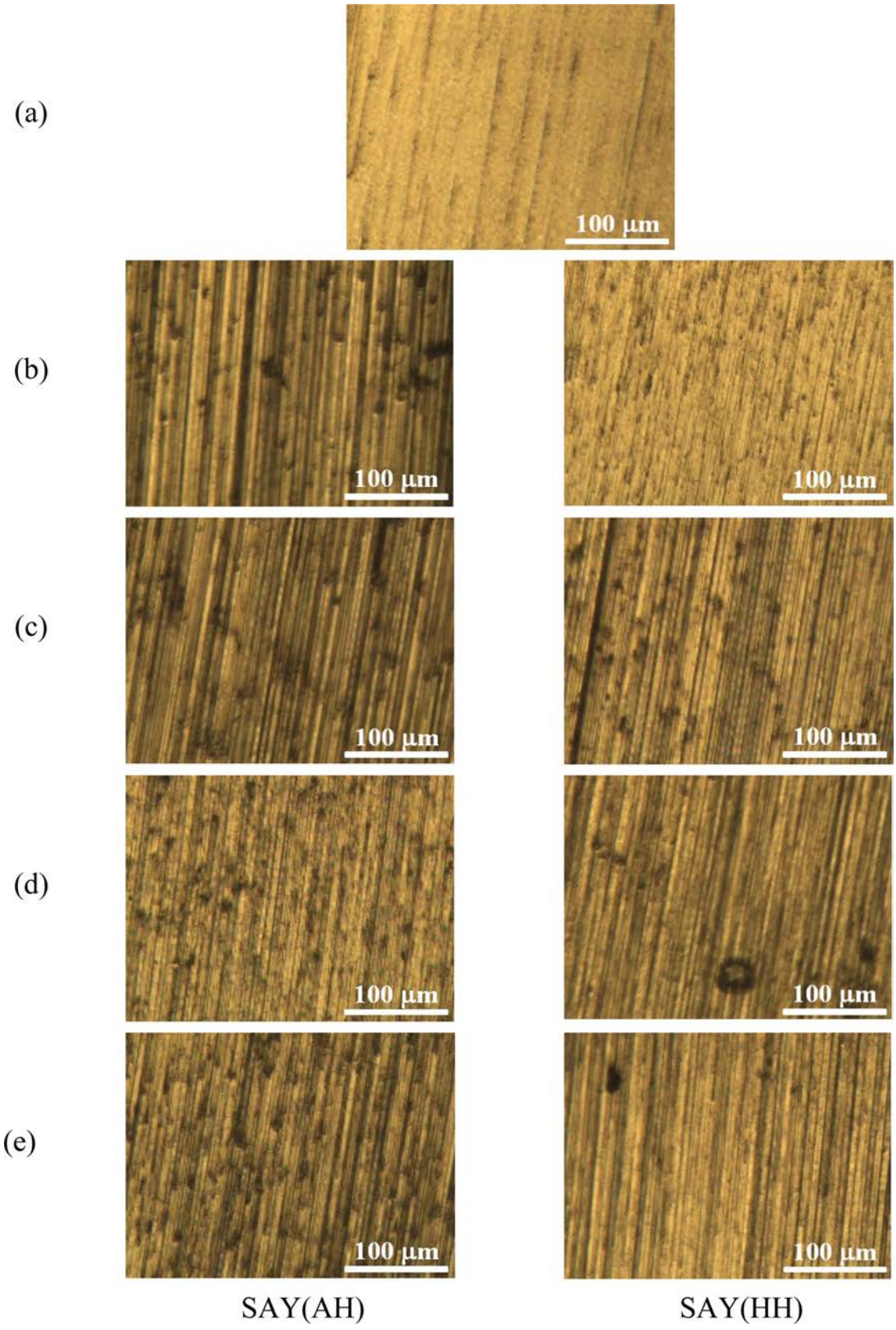

Fig. 1. Optical microscope image of wear part of SAY(AH) and SAY(HH). (a) As-received, (b) 900 ºC, (c) 1000 ºC, (d) 1100 ºC, (e) 1200 ºC.

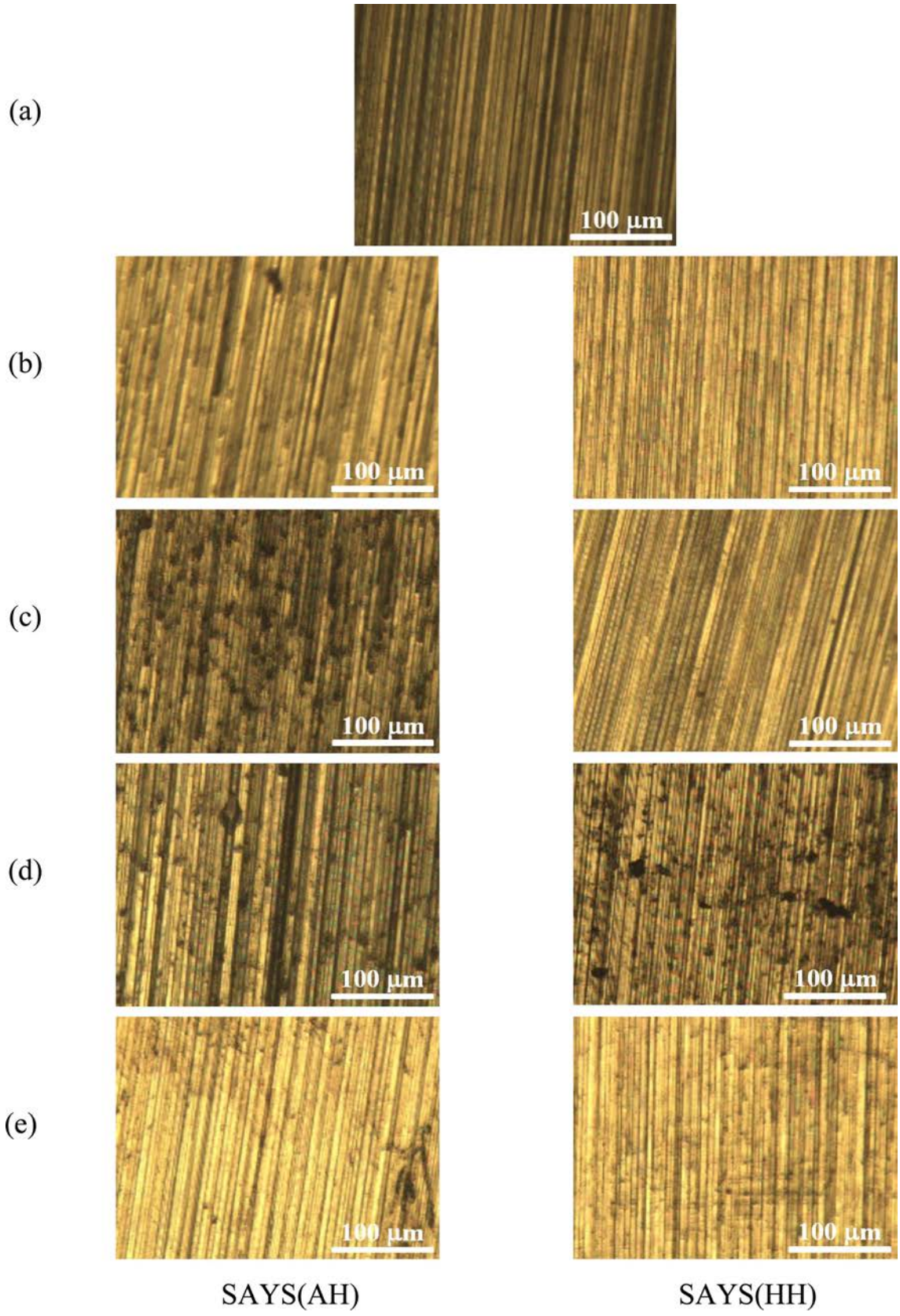

Fig. 2. Optical microscope image of wear part of SAYS(AH) and SAYS(HH). (a) As-received, (b) 900 °C, (c) 1000 °C, (d) 1100 °C, (e) 1200 °C.

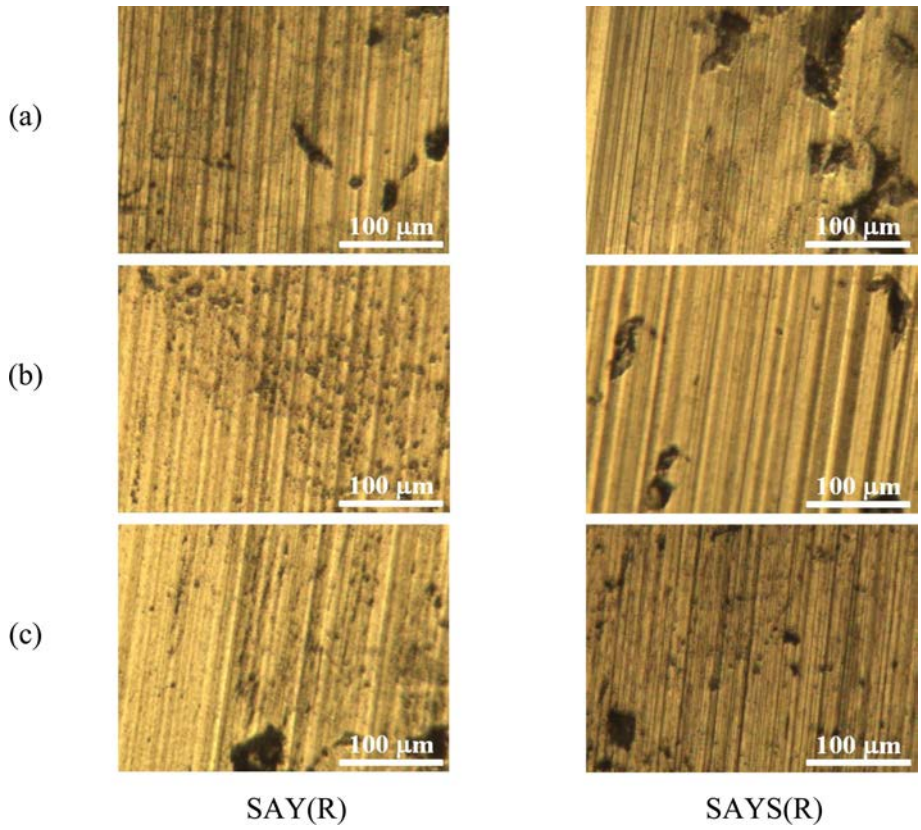

Fig. 3. Optical microscope image of wear part of SAY(R) and SAYS(R). (a) 1100 °C-1 hr, (b) 1100 °C-3 hr, (c) 1100 °C-10 hr.

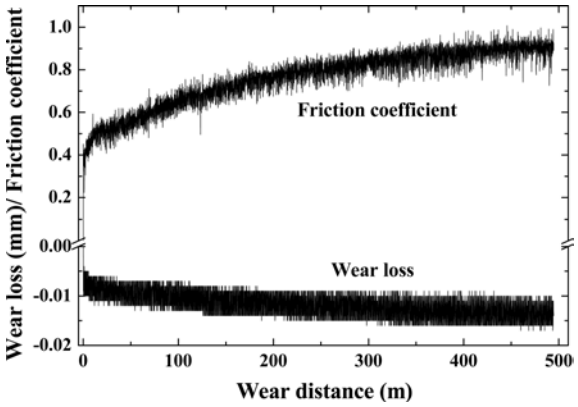

Fig. 4. Typical example of friction coefficient and wear loss for wear distance in as-received specimen.

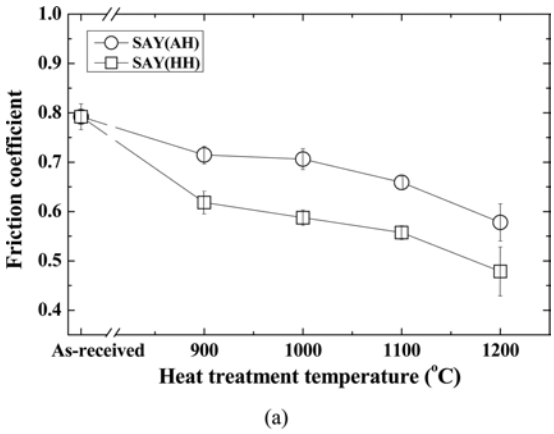

(a)

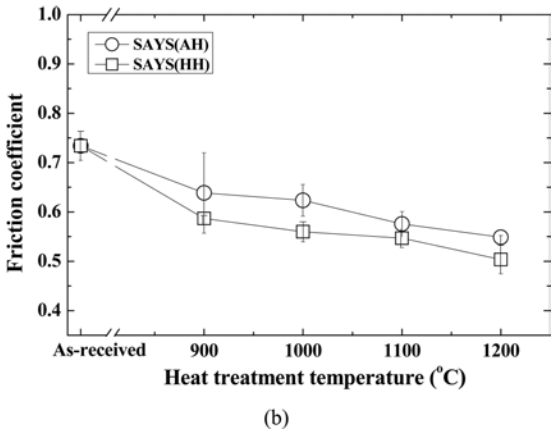

(b)

Fig. 5. Relation between heat treatment temperature and friction coefficient. (a) SAY, (b) SAYS.

flat. The wear loss is measured by the depth of the gap of the specimen as it differs from before and after the wear test by a dial gage. This is closely related to the amount of wear.

Figs. 5(a-b) show the friction coefficient according to the heat treatment temperature of the as-received specimen. Fig. 5(a-b) show SAY and SAYS, respectively. Regardless of the addition of the SiO_2 powder, two kinds of specimens decreased the friction coefficient according to an increase of the heat treatment temperature. All of the heat treated specimens showed a smaller friction coefficient than that of the as-received specimen. The high temperature heat treated as-received specimens

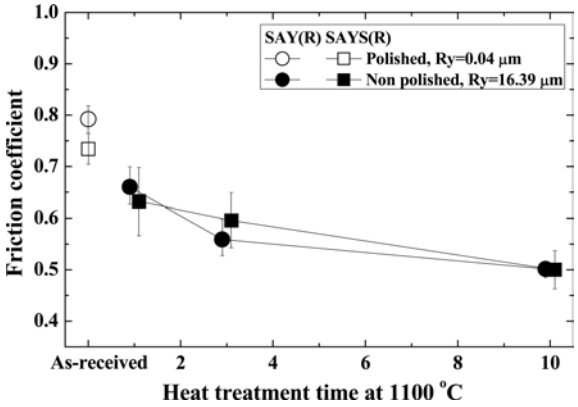

Fig. 6. Friction coefficient according to different heat treatment time at 1100? with different surface roughness specimen.

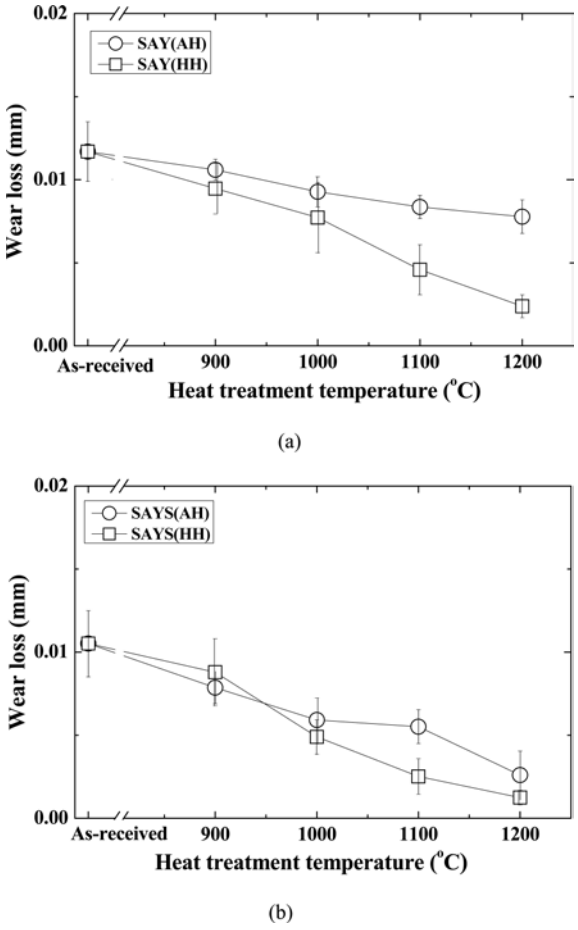

Fig. 7. Relation between heat treatment temperature and wear loss. (a) SAY, (b) SAYS.

(SAY(HH) and SAYS(HH)) showed a lower friction coefficient than that of the as-received specimen (SAY(AH) and SAYS(AH)). This is consistent with a decrease in the friction coefficient at above about 400-500 ºC, a result found in studies by Hannink et al using Al_2O_3 and MgO/ZrO_2. Gyimah et al also reported that the friction coefficient decreased with increasing friction and wear temperature.

Fig. 6 shows the friction coefficient of the heat

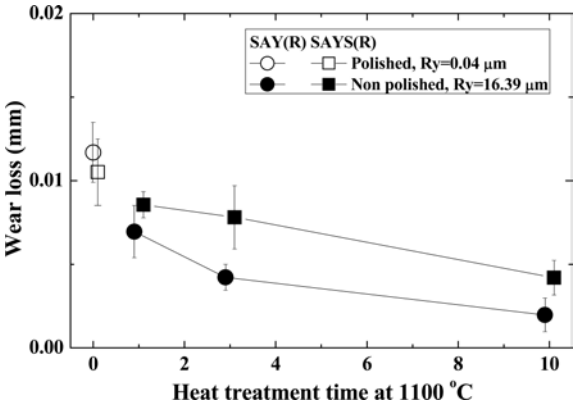

Fig. 8. Wear loss according to different heat treatment time at 1100 ºC with different surface roughness specimen.

treated surface roughness specimen for 1, 3, and 10 hrs at 1100 ºC. The friction coefficient of the mirror polished specimen and the unpolished specimens were almost similar, but the friction coefficient was small as the heat treatment time increased.

Houjou et al sintered Si_3N_4, SiC and Y_2O_3 and heat treated at temperatures between 800 and 1500 ºC for 1, 10 and 100 hrs. In the silicon nitride composite ceramics, an oxide layer was formed on the surface by the heat treatment, and the thickness of the oxide layer became thicker as the temperature and time of the heat treatment became longer. In this study, the heat treated specimens (SAY(AH), SAYS(AH)) for 1 hour at 900 ~ 1200 ºC and the heat treated specimens (SAY(HH), SAYS(HH)) for 1 hr at 1100 ºC using the previous specimen were used. The oxide layer of the heat treated ceramic under these conditions is acting as a lubrication so that the friction coefficient became smaller.

Fig. 7(a-b) show the friction loss according to the heat treatment temperature of the as-received specimen. Fig. 7(a-b) show SAY and SAYS, respectively. The wear loss showed the same tendency as the friction coefficient. Regardless of the addition of the SiO_2 powder, two kinds of specimens decreased the wear loss according to an increase of the heat treatment temperature. All of the heat treated specimens showed a smaller wear loss to that of the as-received specimen. The high temperature heat treated as-received specimens (SAY(HH) and SAYS(HH)) showed lower wear loss compared with the as-received specimen (SAY(AH) and SAYS(AH)). This is because the oxide produced on the surface served as a lubricant.

Fig. 8 shows the wear loss of the heat treated surface roughness specimens for 1, 3, and 10 hrs at 1100 ºC. The wear loss of the two types of mirror polished specimens was similar, but the non-polished specimens were different. That is, the wear loss of the specimen with the SiO_2 powder was large. The authors evaluated the strength and heat treatment characteristics of the SiC by heat treatment a sintered material mixed with

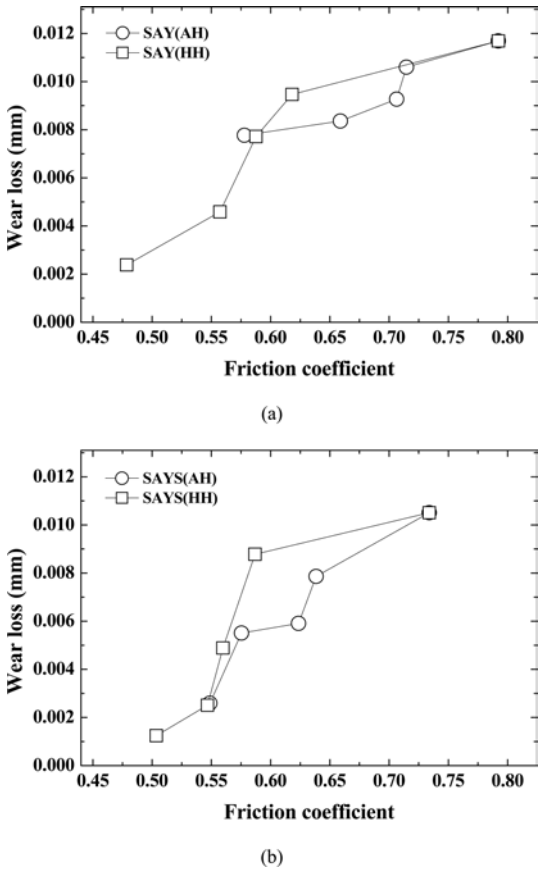

Fig. 9. Relation between friction coefficient and wear loss. (a) SAY, (b) SAYS.

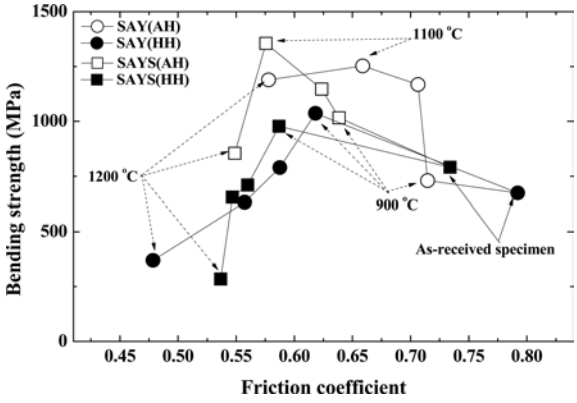

Fig. 10. Relation between friction coefficient and bending strength.

SiO_2 colloid. According to these results, it was confirmed that the SiO_2 was detected on the surface by heat treatment at 1100 °C for 1 hr. Thus, in this study, it is considered that the lubrication effect increased by glassy SiO_2 formed on the surface by the heat treatment, but the wear loss increased.

The relationship between the friction coefficient and the wear loss is shown in Fig. 9(a-b), showing SAY and SAYS, respectively. It can be seen that, the larger the friction coefficient is, the more the wear loss is

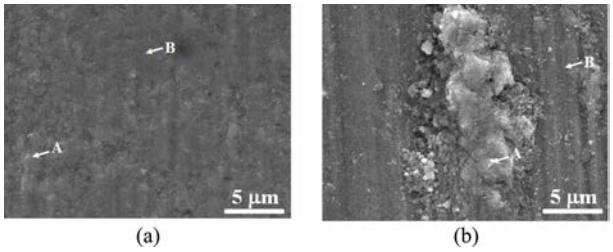

Fig. 11. SEM of wear scars. (a) SAY(A), (b) SAYS(A).

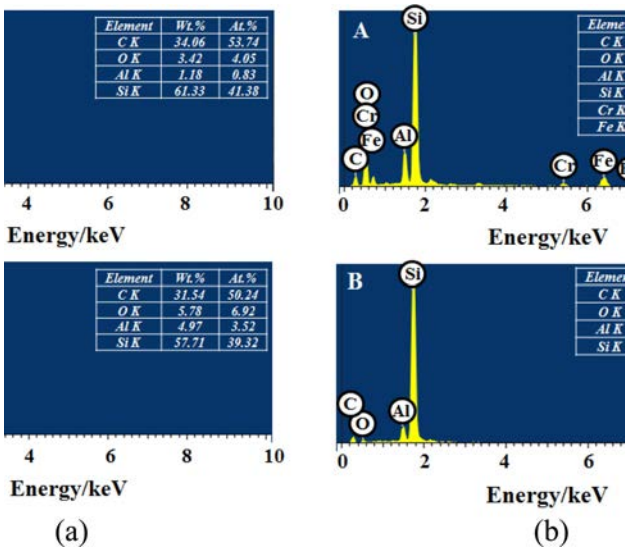

Fig. 12. EDX results of light gray regions (denoted as A) and dark gray regions (denoted as B). (a) SAY(A), (b) SAYS(A).

increased. In addition, the wear loss of the heat treated specimen (SAY(HH), SAYS(HH)) for 1 hr at 1100 °C was slightly larger than that of the as-received specimen (SAY(AH), SAYS(AH)). This phenomenon was slightly larger for SAYS specimens with SiO_2 powder. This is because the SiO_2 oxide forms extensively on the surface due to the increase of the heat treatment temperature and time, so that the wear loss is large.

Fig. 10 shows the relationship between the bending strength and the friction coefficient. The friction coefficient of the as-received specimens, SAY and SAYS, was as large as 0.73 and 0.79, respectively, but the bending strengths were 670 MPa and 790 MPa, respectively. However, SAY (AH) and SAYS (AH) showed the highest bending strength of 1253 MPa (friction coefficient 0.66) and 1355 MPa (friction coefficient 0.58), respectively, at the heat treatment temperature of 1100 °C. However, the bending strength and friction coefficient decreased at the heat treatment temperature of 1200 °C. The bending strength and friction coefficient of SAY (HH) and SAYS (HH) decreased with an increasing temperature. As mentioned above, as the temperature increases, the oxide layer on the surface becomes thicker, and this acts as a lubricant; therefore, the friction coefficient decreased.

After the wear test, further investigation on the worn

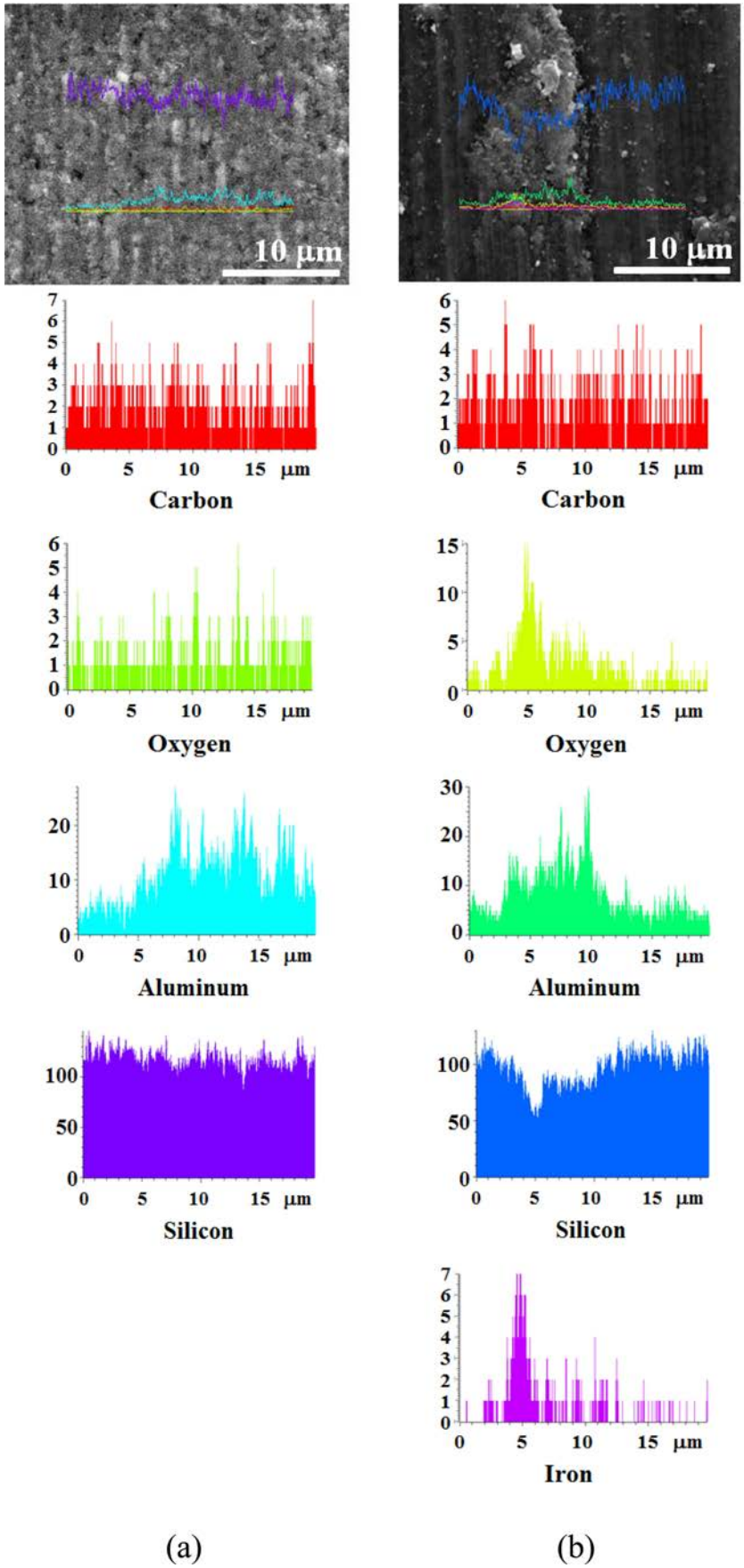

Fig. 13. Line profiles of the transverse sections of the worn surfaces. (a) SAY(A), (b) SAYS(A).

Table 2. Elements of light gray regions and dark gray regions in SAY (At.%).

	SAY(A)		SAY(A) 1100		SAY(H) 1100		SAY(R) 1100 (10 h)	
	A	B	A	B	A	B	A	B
C K	53.74	50.24	58.20	57.30	53.13	55.05	52.65	40.57
O K	4.05	6.92	4.49	2.81	4.84	1.91	6.10	12.80
Al K	0.83	3.52	2.06	0.60	1.09	1.12	1.15	3.73
Si K	41.83	39.32	35.24	39.29	40.94	41.93	40.10	42.90

Table 3. Elements of light gray regions and dark gray regions in SAYS (At.%).

	SAYS(A)		SAYS(A) 1100		SAYS(H) 1100		SAYS(R) 1100(10h)	
	A	B	A	B	A	B	A	B
C K	31.42	49.33	33.12	41.24	40.30	44.61	40.25	52.97
O K	29.68	6.02	40.46	9.70	17.81	7.25	17.51	5.40
Al K	4.46	2.69	1.09	4.87	3.01	4.77	3.28	1.31
Si K	28.18	41.97	16.02	44.19	36.05	43.37	36.43	40.31
Cr K	0.88	–	1.27	–	0.40	–	0.38	–
Fe K	5.38	–	8.05	–	2.42	–	2.15	–

surface morphologies of the specimens were conducted by SEM. Fig. 11(a-b) representatively shows the as-received specimen of SAY and SAYS. Fig. 11(a) SAY can observe scratches on the surface. Fig. 11(b) SAYS can observed the scratches on the surface, there are scattered a large amount of debris combined with indentation defects. This is the result of abrasive adhesion wear. That is, debris was formed by peeling off the surface oxide layer by the addition of the SiO_2. The friction coefficient decreased due to the lubricating action, but a severe micro-cutting phenomenon occurred in the contact surface during the dry sliding process, as the wear loss may be increased by the wear of oxide layer. Besides, the light gray regions (denoted as A) and dark gray regions (denoted as B) were investigated by EDX. Fig. 12 shows the result. The light gray regions and dark gray regions of SAY (Fig. 12(a)) mainly included the C, O, Al and Si elements. The light gray regions of SAYS (Fig. 12(b)) mainly included the C, O, Al, Si, Cr and Fe elements, and the dark gray regions mainly included the C, O, Al and Si elements. The light gray regions of SAYS are the mechanical mixed layer, which were the debris mainly peeled from the counterpart steel ball and subsequently transferred onto the sample; it then underwent a complex formation process of fragmentation, mixing, accumulation, oxidation, and compaction, etc. The elements of the light gray regions and dark gray regions of SAY and SAYS are summarized in Tables 2 and 3.

Fig. 13 shows the line profiles of the cross-sections of the SAY (A) and SAYS (A) specimens. It can be seen that SAY(A) (Fig. 13(a)) can observe the bumpy wear surface and pores, and the longitudinal wear line is disconnection. Si was uniformly detected at the measurement distance (20 mm), and C and O were also obtained relatively uniformly. However, Al was detected more in the convex part than in the concave part. SAYS(A) (Fig. 13(b)) showed a thick wear line and wear debris was observed. The SiO_2 oxide that formed on the surface layer acted the lubrication action and the pores seen in SAY (A) was not observed. The Debris region is composed of oxide micro particles, and is considered to be mechanically mixed by friction wear and the like. Si was detected the low amount in debris consisting of oxide particles; in particular, it obtained the least amount at 5 μm point. On the other hand, the highest amount of O and Fe was detected and it was judged that Fe oxide was formed. A lot of Al was detected in the debris between 2-11 μm. C was uniformly obtained in a measured distance. Ceramic materials are generally subjected not only to brittle fracture under high or impact loads, but also to fatigue cracking induced mainly at grain boundaries by the high surface temperatures and cyclic stresses generally attained under dry sliding conditions. Under the reciprocating sliding process, the grains beneath the metal mixed particles were fractured, thereby resulting in the formation of micro cracks beneath the metal mixed particles. When the micro cracks propagated, connected and deflected to the worn surface, the plate-like metal mixed particles was peeled out from the worn surface and serious wear happened.

Conclusions

This study evaluated the friction wear characteristics according to heat treatment conditions and surface roughness using sintered silicon carbide ceramics. The

conclusion was as follows: based on the observations of the worn surface, transvers section, and wear debris of specimens, the SiC ceramics mainly had abrasive, adhesive and plowing wear during dry sliding. The heat treated as-received specimens and the high temperature heat treated as-received specimens decreased in friction coefficient and wear loss with an increasing heat treatment temperature. This tendency was reduced more than the heat treated as-received specimens in the high temperature heat treated as-received specimens. The friction coefficient of the heat treated surface roughness specimen was not influenced by the roughness, but wear loss was large at high roughness. The higher the heat treatment temperature and the longer the time it was administered, the thicker the SiO_2 oxide that was formed on the surface; thus, the friction coefficient was smaller due to the lubrication action, but the wear loss was larger.

Acknowledgments

This work was supported by the Jungwon University Research Grant(2017-034).

References

1. R.H.J. Hannink, M.J. Murray, and H.G. Scott, Wear 100 (1984) 355-366.
2. G.K. Gyimah, D. Chen, P. Huang, G.C. Barber, Int. J. Sci. Eng. Research 4 (2013) 826-832.
3. S. Jahanmir, “Friction and Wear of Ceramics”, CRC Press (1993) p. 3-12.
4. I. Hutchings, and P. Shipway, “Tribology: friction and wear of engineering materials”, Elsevier (Second Edition, 2017) p. 58-63.
5. S.H. Ahn, and K.W. Nam, Transactions of the KSME(A) 38 (2014) 1117-1123.
6. K.W. Nam, J. Ceram. Process. Res. 13 (2012) 571-574.
7. B. Rigaut, Y.M. Chen, and J.S. Chely, J. Soc. Tribologists and Lubrication Engineers 50 (1994) 485-489.
8. M. Chen, K. Kato, and K. Adachi, Wear 250 (2001) 246-255.
9. P. Andersson, and A. Blomberg, Wear, 170 (1993) 191-198.
10. W. Kanematsu, Y. Yamauchi, T. Ohji, S. Ito, and K. Kubo, J. Ceram. Soc. Japan. 100 (1992) 775-779.
11. K.W. Nam, J. Ceram. Process. Res. 11 (2010) 471-474.
12. M. Ono, W. Nakao, K. Takahashi, and K. Ando, Fatigue Fract. Eng. Mater. Struct. 30 (2007) 1140-1148.
13. K.W. Nam, Trans. Korean Soc. Mech. Eng. A 40 (2016) 263-273.
14. K.W. Nam, and J.R. Hwang, J. Mech. Sci. Technol. 26 (2012) 2093-2096.
15. K. Houjou, and K. Takahashi, Int. J. Struct. Integrity 3 (2012) 41-52.
16. K.W. Nam, H.R. Jeong, J.W. Kim, and S.H. Ahn, J. Ceram. Process. Res. 17 (2016) 1188-1191.
17. K.W. Nam, and E.S. Kim, Mater. Sci. Eng A 547 (2012) 125-127.
18. K.W. Nam, J.S. Kim, and S.W. Park, Mater. Sci. Eng. A 527 (2010) 5400-5404.
19. S.K. Lee, W. Ishida, S.Y. Lee, K.W. Nam, and K. Ando, J. Eur. Ceram. Soc. 25 (2005) 569-576.
20. K.W. Nam, S.H. Park, and J.S. Kim, J. Ceram. Process. Res. 10 (2009) 497-501.
21. K. Houjou, K. Ando, S.P. Liu, and S. Sato, J. Eur. Ceram. Soc. 24 (2004) 2329-2338.